

Published in final edited form as:

*Langmuir*. 2010 June 1; 26(11): 8589–8596. doi:10.1021/la904678p.

## Enhanced Tumor Cell Isolation by a Biomimetic Combination of E-selectin and anti-EpCAM: Implication for Effective Separation of Circulating Tumor Cells (CTCs)

Ja Hye Myung<sup>1,†</sup>, Cari A. Launier<sup>2,†</sup>, David T. Eddington<sup>2</sup>, and Seungpyo Hong<sup>\*,1,2</sup>

<sup>1</sup>Department of Biopharmaceutical Sciences, University of Illinois, Chicago, IL 60612

<sup>2</sup>Department of Bioengineering, University of Illinois, Chicago, IL 60612

### Abstract

Selective detection of circulating tumor cells (CTCs) is of significant clinical importance for the clinical diagnosis and prognosis of cancer metastasis. However, largely due to the extremely low number of CTCs (as low as one in 10<sup>9</sup> hematologic cells) in the blood of patients, effective detection and separation of the rare cells remain a tremendous challenge. Cell rolling is known to play a key role in physiological processes such as recruitment of leukocytes to sites of inflammation and selectin-mediated CTC metastasis. Furthermore, as CTCs typically express epithelial-cell adhesion molecule (EpCAM) on the surface whereas normal hematologic cells do not, substrates with immobilized antibody against EpCAM may specifically interact with CTCs. In this paper, we created biomimetic surfaces functionalized with P- and E-selectin and anti-EpCAM that induce different responses of HL-60 (used as a model of leukocytes in this study) and MCF-7 (a model of CTCs) cells. HL-60 and MCF-7 cells showed different degrees of interaction with P-/E-selectin and anti-EpCAM at a shear stress of 0.32 dyn/cm<sup>2</sup>. HL-60 cells exhibited rolling on P-selectin-immobilized substrates at a velocity of 2.26 ± 0.28 μm/sec whereas MCF-7 cells had no interaction with the surface. Both cell lines, however, showed interactions with E-selectin, and the rolling velocity of MCF-7 cells (4.24 ± 0.31 μm/sec) was faster than that of HL-60 cells (2.12 ± 0.15 μm/sec). On the other hand, only MCF-7 cells interacted with anti-EpCAM-coated surfaces, forming stationary binding under flow. More importantly, the combination of the rolling (E-selectin) and stationary binding (anti-EpCAM) resulted in substantially enhanced separation capacity and capture efficiency (more than 3-fold enhancement), as compared to a surface functionalized solely with anti-EpCAM which has been commonly used for CTC capture. Our results indicate that cell-specific detection and separation may be achieved through mimicking the biological processes of combined dynamic cell rolling and stationary binding, which will likely lead to a CTC detection device with significantly enhanced specificity and sensitivity without any complex fabrication process.

### INTRODUCTION

Although recent advances in diagnostic and therapeutic methods to treat primary tumors hold promise to decrease mortality of cancer, metastasis of cancer still poses a great challenge as patients often relapse.<sup>1-4</sup> Disseminated and circulating tumor cells (DTCs and CTCs),

\* All correspondence should be addressed to: Department of Biopharmaceutical Sciences College of Pharmacy The University of Illinois at Chicago 833 S. Wood St. Rm 335 Chicago, IL 60612 .

† Both authors contributed equally to this work.

Supporting Information Available Supplementary Figure 1 shows fluorescence images of functionalized surfaces treated with E-selectin, anti-EpCAM, and E-selectin/anti-EpCAM mixture at various ratios. This information is available free of charge via the Internet at <http://pubs.acs.org/>.

respectively) are known to induce secondary tumor formation at distant sites from primary tumors, known as metastasis.<sup>5-7</sup> The process of metastasis is not fully understood but one of the most plausible mechanisms involves a similar process of leukocyte homing, i.e. a naturally occurring cell rolling process.<sup>8</sup> Rolling cells then firmly attach to the endothelial layers, followed by transmigration through the endothelium (diapedesis) to form secondary tumors.<sup>9</sup> Thus, research efforts on diagnosis and prognosis of metastatic cancer have been concentrated on detection of DTCs in bone marrow (BM) and CTCs in blood.<sup>10</sup> Detection of DTCs for prognosis studies along with therapeutic treatments requires repeated samplings of BM that is invasive, time-consuming, and often painful for the patients.<sup>11, 12</sup> Consequently, effective detection of CTCs in peripheral blood of cancer patients holds a promise as an alternative due to its minimally invasive and easy sampling procedures (i.e. blood drawing). However the clinical usage of CTCs has not yet been implemented for routine clinical practice because CTCs are extremely rare and estimated to be in the range of one tumor cell in the background of  $10^6$ - $10^9$  normal blood cells.<sup>13, 14</sup>

To date, most methods for CTC detection are based on immunofluorescence labeling using CTC markers such as epithelial-cell-adhesion-molecule (EpCAM).<sup>10, 15</sup> Recent progress in this field includes the development of an automated enrichment and immunocytochemical detection system for CTCs (CellSearch™, Veridex, LLC) that has been approved by the Food and Drug Administration (FDA) for clinical use in metastatic breast cancer patients.<sup>16, 17</sup> Although reliable and stable, the CellSearch™ system has limitations such as complicated sample processing with additional steps needed for plasma removal and magnetic antibody labeling and limited sensitivity with a median 1.2 cells/mL detected from patients with metastatic cancer. Another promising technology for CTC detection and isolation has been recently published by Nagrath et al. using a microfluidic device containing 78,000 anti-EpCAM coated microposts which has increased its sensitivity and specificity for CTC capturing.<sup>18</sup> The CTC-chip does not require multiple processing steps in sample preparation and has shown enhanced sensitivity as compared to the CellSearch™ with a median of 67 cells/mL detected from whole blood samples of patients under comparable conditions.<sup>19</sup> The combined effect of anti-EpCAM-based specificity and the micropost-enhanced hydrodynamic efficiency enabled a capturing of over 60%. However, the enhanced hydrodynamic efficiency relying on the microposts limits the utility of the device at higher flow rates where a significant decrease in the capture efficiency has been observed.

The formation of transient ligand-receptor interactions occurs commonly between cells flowing in the blood and the vascular endothelium; this physiological process is known as cell rolling.<sup>20</sup> Cell rolling plays a key role in biologically important processes such as recruitment of leukocytes to sites of inflammation, homing of hematopoietic progenitor cells, and CTC-induced metastasis. This behavior is typically mediated by dynamic interactions between selectins (E- and P-selectins) on the vascular endothelial cell surface and membrane ligands on the carcinoma cell surface. Endothelial (E)-selectin (CD62E) is particularly noteworthy in disease by virtue of its expression on activated endothelium and on bone-skin microvascular linings, and many studies point to the key role played by E-selectin in being involved in the adhesion and homing of various types of cancer cells such as prostate,<sup>21</sup> breast,<sup>22, 23</sup> and colon<sup>24</sup> carcinoma cells. Thus, tumor cell separation based on the selectin-mediated cell rolling behavior is being pursued as it mimics a physiological process, and eliminates labeling and label removal steps that are necessary for other immune-labeling detection methods.<sup>25</sup> Recently, a tube-type flow chamber that is co-immobilized with E-selectin and tumor necrosis factor-related apoptosis-inducing ligand (TRAIL) achieved concurrent dual functions of inducing rolling and apoptosis of various cell lines.<sup>26</sup> However, given that a large class of cells, including leukocytes, platelets, neutrophils, mesenchymal and hematopoietic stem cells, and metastatic cancer cells all exhibit rolling on selectins, detection that is solely based on cell

rolling has limitations for achieving sufficient specificity, which has hindered translation of the technology to a clinically significant device.

The specific capturing and potential enrichment of CTCs using anti-EpCAM and selectin, respectively, inspired a biofunctionalized surface that mimics biological complexity may detect and isolate target cells at a greater sensitivity and specificity. This concept is supported by the initial physiological interactions between CTCs and endothelium in the bloodstream, which include concurrent rolling and stationary binding steps. Towards this aim, we investigated the following: i) two proteins with distinct biofunctions (selectin to induce rolling and anti-EpCAM to statically capture target cells) can be co-immobilized; ii) a combined rolling and stationary binding can be induced by the mixture of the proteins; and iii) the biomimetic combination enhances overall capture efficiency of the surface. In this paper, these are tested using biofunctional surfaces with immobilized selectins and anti-EpCAM. The surfaces are characterized by X-ray photoelectron scattering (XPS) and fluorescence microscopy using fluorophore-conjugated antibodies. As a proof-of-concept study for the hypothesis of enhanced separation capacity and capture efficiency using protein mixtures, the surfaces are tested using *in vitro* cell lines (MCF-7 cells as a CTC model and HL-60 cells as a leukocyte model) under flow conditions. The effects of the combination of rolling (E-selectin) and stationary binding (anti-EpCAM) on capture efficiency are compared to a surface functionalized solely with anti-EpCAM or selectins. Here we report, for the first time to our knowledge, that combination of dynamic rolling and stationary binding significantly enhances capture efficiency of target cells, which holds great promise to develop a simple, effective device for CTC detection.

## EXPERIMENTAL

### Materials

Recombinant human P-selectin/Fc chimera (P-selectin), E-selectin/Fc chimera (E-selectin), anti-human EpCAM/TROP1 polyclonal antibody (anti-EpCAM), fluorescein-conjugated mouse monoclonal anti-human E-selectin (fluorescein-anti-E-selectin), and allophycocyanin (APC)-conjugated mouse monoclonal anti-human EpCAM/TROP1 (APC-anti-EpCAM) were all purchased from R&D systems (Minneapolis, MN). Unconjugated goat anti-Human IgG (H + L) was acquired from Pierce biotechnology, Inc (Rockford, IL). The epoxy-functionalized glass surfaces (SuperEpoxy2®) were purchased by TeleChem International, Inc (Sunnyvale, CA). All other chemicals were obtained from Sigma-Aldrich (St. Louis, MO) and used without further purification.

### Surface functionalization by immobilization of adhesive proteins

All individual proteins and/or mixture of P-selectin, E-selectin, and anti-EpCAM were immobilized on epoxy functionalized glass surfaces. A general scheme of the surface functionalization via protein immobilization is outlined in Figure 1. The coating areas were defined by a polydimethylsiloxane (PDMS) gasket to confine protein solutions in a desired area, resulting in a clear interface between protein-coated and uncoated regions. For the surfaces functionalized with a single protein, 300  $\mu$ L of each protein (P-selectin, E-selectin, or anti-EpCAM) at a concentration of 5  $\mu$ g/mL in PBS buffer (Cellgro®, without  $\text{Ca}^{2+}$ ,  $\text{Mg}^{2+}$ ) was added on an approximately 2  $\text{cm}^2$  area of a slide defined by a PDMS gasket, followed by incubation at RT for 4 hrs with constant gentle shaking on a plate shaker. The PDMS gasket was then removed, and the whole slide surface was washed with PBS three times. Potential non-specific binding of both protein-coated and uncoated regions was blocked by the final incubation with 1% (w/v) bovine serum albumin (BSA) in PBS buffer (BSA solution). The subsequent experiments using the surfaces were immediately performed, or stored in PBS buffer at 4 °C. Additionally, mixtures of E-selectin and anti-EpCAM were immobilized at various ratios under the same condition described above. A fixed concentration of anti-EpCAM

at 10  $\mu\text{g}/\text{mL}$  was used with various amounts of E-selectin. The final total weights (in  $\mu\text{g}$ ) of anti-EpCAM and E-selectin were 1.5:0, 1.5:0.3, 1.5:1.5, and 1.5:7.5.

### Characterization of the functionalized surfaces by fluorescence microscopy

The co-immobilization process of anti-EpCAM and E-selectin was characterized using APC-anti-EpCAM and fluorescein-anti-E-selectin, respectively. The surfaces functionalized with P-selectin was explicitly characterized previously.<sup>27</sup> As neither fluorophore-tagged EpCAM nor fluorescent secondary antibody specific to anti-EpCAM is commercially available, APC-anti-EpCAM was co-immobilized with E-selectin, and red fluorescence was observed from the surface. For detection of E-selectin, anti-EpCAM/E-selectin-immobilized slides were incubated with fluorescein-conjugated anti-E-selectin (25  $\mu\text{g}/\text{mL}$ ) at 4 °C for 1 hr, followed by a washing step (three times using PBS buffer). All slides were then mounted using Vectashield® mounting medium (Vector laboratories, Inc., Burlingame, CA), and air bubbles in the mounting medium were gently removed by applying pressure to the cover slides. The fluorescence images were taken using an Olympus IX70 inverted microscope equipped with a fluorescence illuminator (IX 70-S1F2, Olympus America, Inc., Center Valley, PA) using a 10 $\times$  objective, a CCD camera (QImaging Retiga 1300B, Olympus America, Inc.) and filters for FITC (450 nm excitation and 535 nm emission) and APC (560 nm excitation and 645 nm emission). For each image (triplicate for each sample), 5 regions of equal size were randomly selected, and the total pixel intensity values within these regions were acquired using ImageJ (NIH). The slide treated with the BSA solution was used as background and its intensity value was subtracted from all sample slides. The intensities obtained from the protein mixture-immobilized slides were normalized based on those functionalized with a single protein (anti-EpCAM or E-selectin) to compare the relative amounts.

### Characterization of the surfaces by X-ray photoelectron spectroscopy (XPS)

Protein-immobilized surfaces were characterized by XPS.<sup>27</sup> XPS measurements were performed using an Axis 165 X-ray photoelectron spectrometer (Kratos Analytical, Manchester, U.K.) equipped with a monochromatic AlK $\alpha$  source ( $h\nu = 1486.6$  eV, 150W) and a hemispherical analyzer. The % mass concentrations were obtained from high-resolution spectra of the C 1s, O 1s, N 1s, and S 2p regions at an X-ray irradiating angle of 30° with pass energy of 80 eV and a step size of 0.5 eV, carried on 5 scans per each spectrum.

### Cell lines

HL-60 and MCF-7 cells were purchased from ATCC (Manassas, VA). *Discosoma sp.* Red fluorescent protein (DsRED)-transfected MCF-7 (DsRED-MCF-7) cells that were transfected using an HIV-1-based lentiviral vector<sup>28</sup> were a generous gift of Prof. William Beck at UIC.

HL-60 cells were cultured in IMDM media supplemented with 20% (v/v) fetal bovine serum (FBS) and 1% (v/v) penicillin/streptomycin in a humidified incubator at 37 °C and 5% CO<sub>2</sub>. MCF-7 cells and DsRED-MCF-7 cells were cultured in DMEM media that were supplemented with 10% (v/v) FBS and 1% (v/v) penicillin/streptomycin under the same condition of incubation for HL-60 cells. Prior to cell culture, to enrich the transfected (fluorescent) cell population, DsRED-MCF-7 cells were isolated from non-transfected MCF-7 cells via dilution of cell suspension (10<sup>3</sup> cells in 10 mL of media in a petri dish) and selection of the transfected MCF-7 cells using a fluorescence microscope (Olympus IX70). HL-60, MCF-7, and DsRED-MCF-7 cells were prepared by resuspension in their own supplemented media with anti-IgG and kept on ice during the subsequent cell rolling experiments.<sup>29</sup>

## Flow chamber experiments

A typical flow chamber experiment was performed as following. A glass slide functionalized by protein immobilization, a gasket (30 mm (L) × 10mm (W) × 0.25 mm (D), Glycotech, Gaithersburg, MD), and a rectangular parallel plate flow chamber (Glycotech) were assembled in line under vacuum. To observe cellular interactions with the biofunctionalized surfaces, individual cell lines (HL-60 or MCF-7) as well as mixtures of the two cell lines (HL-60 and DsRED-MCF-7) at a concentration between  $10^5$  and  $10^7$  cells/mL were injected into the flow chamber at various flow rates (0.08-1.28 dyn/cm<sup>2</sup>) using a syringe pump (New Era pump Systems Inc., Farmingdale, NY). Note that, in this flow chamber, 200  $\mu$ L/min of flow rate is correspondent to 0.32 dyn/cm<sup>2</sup> of a wall shear stress,  $32 \text{ s}^{-1}$  of a wall shear rate, and 80  $\mu$ m/sec of near-wall non-adherent cell velocity according to the Goldman equation.<sup>30</sup>

## Observation of cellular responses on various functional surfaces

Throughout this study, the cellular behaviors on the various surfaces in the flow chamber were all monitored using the Olympus IX70 microscope and images were recorded using a CCD camera. Rolling velocities of cells on the immobilized proteins were calculated based on the images taken every second for 1 min, using ImageJ. Cell rolling was defined when the rolling velocities were less than 50% of the free stream velocity (e.g. slower than 40  $\mu$ m/sec at a flow rate of 200  $\mu$ L/min). Rolling dynamic data was presented as mean  $\pm$  standard error of the mean (SEM) values of repetitive observations. To confirm the statistical significance between data points, the rolling velocities of more than 40 cells per image were tracked in independent at least 5 replicates.

To evaluate separation of the two cell populations in the mixtures, fluorescent DsRED-MCF-7 cells were used as a CTC model so that they could be easily distinguished from the non-fluorescent leukocyte model (HL-60 cells) in a 50:50 mixture. The surface interactions of the cell mixture on each type of proteins, as well as the cell separation at the interface between E-selectin (left) and anti-EpCAM (right)-coated regions were visualized using the fluorescent and bright fields for 1 min. The merged images of the fluorescent and bright fields were taken in the absence of the flow.

The DsRED-MCF-7 capture efficiency of the surfaces functionalized with E-selectin/anti-EpCAM combinations was measured as follows. The slides functionalized with the different ratios of E-selectin/anti-EpCAM combinations were prepared, and DsRED-MCF-7 cells (suspended in PBS at 2,500 cells/mL with anti-IgG) were injected into a flow chamber, followed by repetitive syringe pushing in and withdrawing at 100  $\mu$ L/min (0.16 dyn/cm<sup>2</sup>). The numbers of captured cells on a pre-defined area of protein-immobilized surface were counted using a microscope at each cycle. A cycle consisting of forward flow (pushing) for 2.5 min, and backward flow (withdrawing) for 2.5 min, and PBS washing for 1 min. As the known number of DsRED-MCF-7 cells was perfused into the flow chamber, the number of captured cells could be translated into the capture efficiency (%). The measured capture efficiencies of the protein mixture-immobilized slides were statistically analyzed by comparing to those of the anti-EpCAM-immobilized slides using one-factor ANOVA, followed pair-wise comparisons among levels of weight for post-hoc analyses by Fisher's least significant difference (LSD) tests with 95% simultaneous confidence intervals (SPSS software, Chicago, IL). Prior to the ANOVA test, we also confirmed that all the capture efficiency data are normally distributed based on both Kolmogorov-Smirnov and Shapiro-Wilk tests using SPSS software. Overall error rate of  $p < 0.05$  was considered statistically significant and marked \* as shown in Figure 6.

## RESULTS

### Confirmation of immobilization of E-selectin, anti-EpCAM, and combinations of the proteins on glass substrates

Surface functionalization by protein immobilization was confirmed by fluorescence microscopy and XPS, as summarized in Tables 1 and 2, respectively. The commercially available epoxy-terminated slides with highly reactive coupling efficiency (via amine/hydroxyl/thiol-based chemistries) and low fluorescence background allowed quantitative and reliable surface analyses using the two techniques. The presence of E-selectin on the surface was observed by immunostaining using fluorescein-anti-E-selectin (green fluorescence). APC-anti-EpCAM (red fluorescence) was used instead of non-fluorescent anti-EpCAM to image the surface immobilized anti-EpCAM by fluorescence microscopy. Table 1 summarizes the measured fluorescence intensities of the various bioadhesive surfaces. For the surfaces functionalized with E-selectin/anti-EpCAM mixtures, the measured fluorescence intensities of each fluorophore well dictate the compositions of each protein. With an increase of the amount of E-selectin immobilized, the green fluorescence intensity was obviously increased, but minimal changes in the red fluorescence intensity were also observed.

The immobilization of anti-EpCAM and/or E-selectin was quantitatively confirmed by an increase in carbon and nitrogen compositions and decreased silicon detection in the underlying glass substrate, as measured by XPS analysis (Table 2). Furthermore, as the amount of immobilized E-selectin in the mixture of anti-EpCAM and E-selectin was increased, the amounts of carbon and nitrogen on the surface were increased with a decreased silicon composition. All surfaces immobilized with proteins had a high degree of coverage, as evidenced by the lack of visible underlying silicon. The measured nitrogen content likely corresponds to the degree of protein coverage on the glass surface, which is supported by the increased nitrogen composition when the total amount of proteins immobilized was increased.

### Interactions of cells on the protein-immobilized surfaces

Cell interactions with the protein-immobilized surfaces under flow were assessed using a commercially available rectangular parallel-plate flow chamber. A breast cancer cell line, MCF-7 was employed as a CTC model. The rolling behavior of the MCF-7 cells was compared with that of HL-60 cells, a human myeloid leukocytic cell line, which expresses a high level of sialyl Lewis<sup>x</sup> and exhibits rolling on selectins mediated primarily by P-selectin glycoprotein-1 (PSGL-1).<sup>31, 32</sup>

Each sets (a and b, c and d, and e and f) of Figure 2 show HL-60 cells on P-selectin, E-selectin, and anti-EpCAM coated surfaces at  $t = 0$  s (a randomly-picked starting recording time during the flow experiment) and 5 s (5 sec after the starting time), respectively. Note that the HL-60 cells on anti-EpCAM-coated slide observed in the images at 0 s were non-adherent cells that were in the main flow but vertically close to the surface. As previously reported, HL-60 cells exhibited stable rolling on both P- and E-selectin-immobilized slides at velocities of  $2.26 \pm 0.28$  and  $2.12 \pm 0.15$   $\mu\text{m}/\text{sec}$ , respectively, under  $0.32$   $\text{dyn}/\text{cm}^2$  of shear stress. HL-60 cells showed no interactions with the immobilized anti-EpCAM, traveling the flow path in the chamber at the speed of free stream velocity (Figure 2e and f). In contrast, as shown in Figure 3, MCF-7 cells did not interact with immobilized P-selectin, but exhibited the rolling response on the E-selectin coated surfaces. The rolling velocities of MCF-7 on E-selectin-immobilized slides ( $4.24 \pm 0.31$   $\mu\text{m}/\text{sec}$ ) were faster than those of HL-60 ( $2.12 \pm 0.15$   $\mu\text{m}/\text{sec}$ ). It should be noted that the rolling velocities of MCF-7 cells varied between experiments with relatively high standard errors, whereas the velocities of HL-60 cells on E-selectin-immobilized slides were relatively consistent between experiments. Unlike HL-60 cells, however, MCF-7 cells exhibited a strong interaction with immobilized anti-EpCAM slides, rolling very slowly ( $0.09$

$\pm 0.03 \mu\text{m}/\text{sec}$ ), so that they appeared to be stationary captured on the surface. Additionally, the rolling velocities of HL-60 and MCF-7 cells on E-selectin were measured at 4 different shear stresses ( $0.08\text{-}1.28 \text{ dyn}/\text{cm}^2$ ) as shown in Figure 4. The rolling velocity of MCF-7 cells was significantly increased with an increase of the shear stress ( $\sim 3.2\text{-}8.0 \mu\text{m}/\text{sec}$ ) whereas the rolling response of HL-60 cells was less dependent upon the flow rate change ( $\sim 1.5\text{-}2.3 \mu\text{m}/\text{sec}$ ).

### **Enhanced separation of tumor cells from two cell populations using combinations of anti-EpCAM and E-selectin**

Interactions of mixtures of the two cell lines with various surfaces functionalized by P-selectin, E-selectin, anti-EpCAM, and combinations of E-selectin/anti-EpCAM were observed under flow conditions, as shown in Figure 5. Note that DsRED-MCF-7 cells were used for easy recognition, as appeared to be red in the all images taken by a fluorescence microscope. As shown in figure 5a, P-selectin induced rolling of HL-60 but did not interact with DsRED-MCF-7 cells, which is consistent with the results using non-transfected MCF-7 cells as shown in Figure 3. E-selectin, on the other hand, caused both cells to roll as presented in Figure 5b. The surface with anti-EpCAM alone induced stationary adhesion of DsRED-MCF-7 cells exclusively. Although HL-60 cells had no interaction with anti-EpCAM, some of them were still located on the images of the anti-EpCAM-immobilized surface (Figure 5c), but these cells were in the bulk flow and not captured on the slide. As shown in Figure 5d, the combined, but spatially separated E-selectin and anti-EpCAM indeed provided an enhanced separation of MCF-7 cells from the cell mixture, compared to the surface functionalized with E-selectin. Both cell types rolled on the E-selectin coated region (the left-hand side of the image), followed by clear separation of the pure MCF-7 cells in the adjacent anti-EpCAM coated region (the right-hand side).

### **Enhanced capturing of tumor cells using combinations of anti-EpCAM and E-selectin**

The effect of E-selectin addition to the anti-EpCAM coated surface was further examined by a quantitative analysis of capture efficiency of DsRED-MCF-7 cells. Figure 6a and b demonstrate a statistically significant enhancement in capture efficiency with the surface immobilized with the mixtures (anti-EpCAM and E-selectin), as compared to the surface with anti-EpCAM only. As shown in Figure 6a and b, the average number of captured cells by the surfaces with the two proteins was enhanced in an E-selectin concentration dependent manner. The enhancement of capture efficiency of the surface with E-selectin/anti-EpCAM compared to one with anti-EpCAM alone was observed to be as high as 3-fold.

To further evaluate cell capture under various conditions, a series of experiments in which DsRED-MCF-7 cells ( $2,500 \text{ cells}/\text{mL}$  of PBS buffer) were spiked with HL-60 ( $2,500 \text{ cells}/\text{mL}$  of PBS buffer) under the presence of anti-IgG was conducted. The rolling velocity of HL-60 cells was measured at a flow rate of  $200 \mu\text{L}/\text{min}$  ( $0.32 \text{ dyn}/\text{cm}^2$ ). Figure 7 quantitatively presents capture efficiency of DsRED-MCF-7 cells and rolling velocities of HL-60 on surfaces with co-immobilized E-selectin and anti-EpCAM at various ratios. As the amount of E-selectin in the total immobilized proteins was increased, the capture efficiency of DsRED-MCF-7 cells was increased, while the rolling velocity of HL-60 cells was decreased.

## **DISCUSSION**

This study investigated three phenomena: i) two proteins with distinct biological functions can be co-immobilized; ii) rolling and stationary binding of tumor cells can be controlled by immobilized proteins; and iii) the protein combination enhances overall capture efficiency of tumor cells.

Tables 1 and 2 demonstrate co-immobilization of the two proteins. The red fluorescence from APC and the green fluorescence from fluorescein from the surfaces immobilized with either anti-EpCAM or E-selectin have little to no spectral overlap (supplementary figure 1). Furthermore, the even distribution of detected fluorescence (supplementary figure 1) indicates that uniform immobilization of both anti-EpCAM and E-selectin was achieved. The specific correlation between fluorescence and protein presentation on the slides was confirmed by two experiments. First, the control surfaces treated with BSA exhibited neither red nor green fluorescence, indicating that non-specific protein adsorption was minimal, which is consistent with a previous report.<sup>33</sup> Second, although E-selectin/APC-anti-EpCAM combinations showed a slightly decreased red fluorescence intensities (by ~30%) compared to the surfaces functionalized solely with anti-EpCAM at the same concentration, the decrease was marginal. By way of contrast, the green fluorescence intensities from fluorescein-anti-E-selectin substantially increased, in a non-linear fashion, with an increase of the immobilized amount of E-selectin in the protein mixtures.

Rolling and stationary binding were individually assessed to test the second phenomenon. As shown in Figure 2, 3, and 4, we have found that the MCF-7 response on different surfaces can be controlled from no interaction (P-selectin) and the rolling response (E-selectin) to stationary binding (anti-EpCAM). The rolling velocities of the HL-60 cells that have a high level of PSGL-1 or sialyl Lewis X (sLe<sup>x</sup>) expression were less shear stress-dependent than those of the MCF-7 cells (carcinoma cells).<sup>34</sup> It is most likely caused by the regulation mechanisms by which leukocytic cells such as HL-60 maintain constant rolling velocities under varying flow conditions (Figure 4) whereas carcinoma cells do not.<sup>35, 36</sup> Although the transient binding for rolling is a state between firm adhesion and the lack of the adhesion (i.e. no interaction), the rolling of leukocytic cells through selectins is highly stable due to a high density of selectin ligands presented on the leukocytic cells and their resistance against hydrodynamic force applied on the cells.<sup>37</sup> It may be also related to rigidity of cells. One can easily imagine that rigid cells are typically more sensitive to shear stress than deformable cells. As a result, leukocytic cells are known to have a nearly constant rolling speed *in vivo* over a wide range of shear stresses.<sup>38</sup> It is also suspected that leukocytic cells maintain a constant rolling speed by shear dependent compensation mechanisms such as increasing the number of tethers and the number of selectin bonds so that they can be uniformly exposed to activating stimuli.<sup>35</sup> MCF-7 cells (Carcinoma cells), on the other hand, seem to lack these mechanisms, given that they are more susceptible to changes in shear stress (Figure 4). Moreover, the formation of metastatic cancers often exhibits the organ selectivity because of the different interactions between the ligands of cancer cells and the organ-specific selectins of endothelial cells for the extravasation of CTCs, which does not require CTCs to adapt the controlling mechanism of the leukocytic cells.<sup>39</sup>

MCF-7 cells exhibit the rolling behavior only on E-selectin, and as reported by Aigner et al.,<sup>34</sup> MCF-7 cells do not interact with P-selectin. Although MCF-7 cells express CD24, a P-selectin ligand, a lack of decoration with sLe<sup>x</sup> results in weak interactions that are not strong enough to stably support rolling on P-selectin.<sup>34</sup> E-selectin-mediated rolling of MCF-7 cells under flow was reported by Toezeren et al.<sup>40</sup> Under the presence of laminar flow, they reported that the adhesion capacity and rolling behavior of MCF-7 cells on human umbilical endothelial cells (HUVECs) were blocked by treatment with antibody against E-selectin on the surface of HUVECs, without providing clear evidence. We have shown that clear interaction of MCF-7 cells with immobilized E-selectin in Figure 3, and the behavior of MCF-7 cells was compared with HL-60. However, it is still unclear which interaction induces the observed rolling response. As a ligand of MCF-7 cells against E-selectin needs to be identified because MCF-7 cells lack most of the known ligands against E-selectin such as PSGL-1,<sup>34</sup> CD44,<sup>41</sup> and sLex.<sup>34</sup> There have been no definitive reports that clearly identify ligands of MCF-7 cells against E-selectin in the literature.

Adherent proteins that are involved in the metastasis process are randomly co-distributed on the endothelium.<sup>42</sup> Thus, our hypothesis was that cooperation of adherent proteins to trap tumor cells would be more efficient than the activity of one of them alone. The surfaces with the protein mixtures (anti-EpCAM and E-selectin) indeed more efficiently recognize DsRED-MCF-7 cells out of the cell mixture with HL-60 cells than the surfaces functionalized solely with anti-EpCAMs (Figures 5 and 6). The protein combinations used in this study clearly demonstrate great potential to improve sensitivity and specificity of CTC separation and capturing from the whole blood. The capture efficiency achieved in this study is as high as approximately 35%. Enhancing hydrodynamic efficiency of the device will likely further increase the capture efficiency. That is, introduction of turbulent flow in lieu of the laminar flow we used in this study will increase the chance of cells to interact with the surface, thereby maximizing the capture efficiency. It was previously reported that microposts in a microfluidic channel<sup>18</sup> or a chaotic mixer<sup>43</sup> substantially increase interactions between flowing particles (cells) with microfluidic channel surfaces.

One can argue that an increase of E-selectin composition in the protein mixture may lead pre-occupation of the surface by abundant cells such as leukocytes (HL-60 in this study), resulting in binding interruption of CTCs (MCF-7 in our study). However, it would not be the case because HL-60 cells exhibit the continuous dynamic rolling response whereas MCF-7 cells remain statically adhered on the surface. That is, a thorough washing step will remove all the rolling cells, leaving only captured cells behind on the surface. Further, it is shown that the enhanced capture efficiency of MCF-7 cells by addition of E-selectin to anti-EpCAM is not interrupted by competitive binding of HL-60 cells. Instead, it is our expectation that E-selectin would be effective in pulling CTCs (MCF-7 cells in this research) along with leukocytes out of the blood flow, inducing rolling, thereby reducing the velocities of the flowing cells, which would facilitate stationary binding of CTCs by adjacent anti-EpCAM on the surface. Furthermore, given that cells exhibit significantly different rolling velocities and different levels of interactions with various proteins, the surface responses of different types of cells are expected to be easily controlled by various combinations of proteins. Another potential problem of our CTC detection method as a prognostic tool is that tumor cells are known to alter their adhesiveness and expression of various proteins on their surfaces upon therapeutic intervention.<sup>44</sup> If the surface property alterations result in a substantial decrease in the capture efficiency of our device, a mix-and-match approach using various ratios between E-selectin and anti-EpCAM would be necessary. That is, a thorough study on the relationship between surface properties of CTCs during treatments and sensitivity/specificity of various protein combinations should be well understood prior to implementation of this method into clinics.

Taken together, it is obvious that the addition of E-selectin can induce the rolling of various cell types to be readily accessible by anti-EpCAM that recognizes/captures tumor cells, resulting in substantially enhanced capture efficiency of tumor cells by the surface – more than 3-fold enhancement as compared to the surface with anti-EpCAM alone. The E-selectin-induced tumor cell rolling most likely maximizes the chance of the tumor cells to interact with anti-EpCAM on the surface, resulting in effective stationary binding.

## CONCLUSION

We have achieved the evenly distributed, stable immobilization of proteins: P-selectin, E-selectin, anti-EpCAM, and mixtures of the proteins, using epoxy-functionalized glass slides. The immobilized proteins maintained their own biological adhesive functions that induce cell rolling and stationary binding in each specific protein-dependent manner. The patterning and combination of these immobilized proteins as a step towards mimicking physiological complexity can be used to design therapeutic or diagnostic devices for capturing specific cells using their enhanced separation capacity and capture efficiency. We are presently translating

these results to a device to capture CTCs from the mixture of other cell lines and whole blood. In addition to the potential use of this device as a metastatic cancer treatment tool by filtering CTCs from the bloodstream, the advantages of this device include the ability to collect CTCs from whole blood under continuous flow without labeling or damaging the CTCs. Therefore, the collected CTCs can be extracted and potentially be subject of further analysis such as genetic understanding and responses for currently available therapeutic drugs by culture expansion.

## Supplementary Material

Refer to Web version on PubMed Central for supplementary material.

## Acknowledgments

This work was supported by National Science Foundation (NSF) under grant # CBET-0931472. This investigation was conducted in a facility constructed with support from grant C06RR15482 from the NCCR NIH. The authors thank Prof. Richard A. Gemeinhart and his group members for optical/fluorescence microscopy measurements and helpful discussion throughout the work.

## REFERENCES

1. Karnon J, Kerr GR, Jack W, Papo NL, Cameron DA. Health care costs for the treatment of breast cancer recurrent events: estimates from a UK-based patient-level analysis. *Br J Cancer* 2007;97(4): 479–485. [PubMed: 17653077]
2. Dong F, Budhu AS, Wang XW. Translating the metastasis paradigm from scientific theory to clinical oncology. *Clin Cancer Res* 2009;15(8):2588–93. [PubMed: 19351761]
3. Pepper MS. Lymphangiogenesis and tumor metastasis: myth or reality? *Clin Cancer Res* 2001;7(3): 462–8. [PubMed: 11297234]
4. Hüsemann Y, Geigl JB, Schubert F, Musiani P, Meyer M, Burghart E, Forni G, Eils R, Fehm T, Riethmüller G, Klein CA. Systemic spread is an early step in breast cancer. *Cancer Cell* 2008;13(1): 58–68. [PubMed: 18167340]
5. Chiang AC, Massague J. Molecular basis of metastasis. *N Engl J Med* 2008;359(26):2814–2823. [PubMed: 19109576]
6. Cristofanilli M, Budd GT, Ellis MJ, Stopeck A, Matera J, Miller MC, Reuben JM, Doyle GV, Allard WJ, Terstappen LWMM, Hayes DF. Circulating tumor cells, disease progression, and survival in metastatic breast cancer. *N Engl J Med* 2004;351(8):781–791. [PubMed: 15317891]
7. Paget S. The distribution of secondary growths in cancer of the breast. 1889. *Cancer Metastasis Rev* 1989;8(2):98–101. [PubMed: 2673568]
8. Mantovani A, Allavena P, Sica A, Balkwill F. Cancer-related inflammation. *Nature* 2008;454(7203): 436–44. [PubMed: 18650914]
9. Mackay CR. Moving targets: cell migration inhibitors as new anti-inflammatory therapies. *Nat Immunol* 2008;9(9):988–998. [PubMed: 18711436]
10. Riethdorf S, Pantel K. Disseminated tumor cells in bone marrow and circulating tumor cells in blood of breast cancer patients: current state of detection and characterization. *Pathobiology* 2008;75(2): 140–8. [PubMed: 18544969]
11. Alix-Panabieres C, Muller V, Pantel K. Current status in human breast cancer micrometastasis. *Curr Opin Oncol* 2007;19(6):558–63. [PubMed: 17906452]
12. Lacroix M. Significance, detection and markers of disseminated breast cancer cells. *Endocr Relat Cancer* 2006;13(4):1033–67. [PubMed: 17158753]
13. Pantel K, Otte M. Occult micrometastasis: enrichment, identification and characterization of single disseminated tumour cells. *Semin Cancer Biol* 2001;11(5):327–37. [PubMed: 11562175]
14. Zieglschmid V, Hollmann C, Bocher O. Detection of disseminated tumor cells in peripheral blood. *Crit Rev Clin Lab Sci* 2005;42(2):155–96. [PubMed: 15941083]

15. Krivacic RT, Ladanyi A, Curry DN, Hsieh HB, Kuhn P, Bergsrud DE, Kepros JF, Barbera T, Ho MY, Chen LB, Lerner RA, Bruce RH. A rare-cell detector for cancer. *Proc Natl Acad Sci U S A* 2004;101(29):10501–4. [PubMed: 15249663]
16. Danila DC, Heller G, Gignac GA, Gonzalez-Espinoza R, Anand A, Tanaka E, Lilja H, Schwartz L, Larson S, Fleisher M, Scher HI. Circulating tumor cell number and prognosis in progressive castration-resistant prostate cancer. *Clin Cancer Res* 2007;13(23):7053–8. [PubMed: 18056182]
17. Riethdorf S, Fritsche H, Muller V, Rau T, Schindlbeck C, Rack B, Janni W, Coith C, Beck K, Janicke F, Jackson S, Gornet T, Cristofanilli M, Pantel K. Detection of circulating tumor cells in peripheral blood of patients with metastatic breast cancer: a validation study of the CellSearch system. *Clin Cancer Res* 2007;13(3):920–8. [PubMed: 17289886]
18. Nagrath S, Sequist LV, Maheswaran S, Bell DW, Irimia D, Ulkus L, Smith MR, Kwak EL, Digumarthy S, Muzikansky A, Ryan P, Balis UJ, Tompkins RG, Haber DA, Toner M. Isolation of rare circulating tumour cells in cancer patients by microchip technology. *Nature* 2007;450(7173):1235–9. [PubMed: 18097410]
19. Maheswaran S, Sequist LV, Nagrath S, Ulkus L, Brannigan B, Collura CV, Inserra E, Diederichs S, Iafrate AJ, Bell DW, Digumarthy S, Muzikansky A, Irimia D, Settleman J, Tompkins RG, Lynch TJ, Toner M, Haber DA. Detection of mutations in EGFR in circulating lung-cancer cells. *N Engl J Med* 2008;359(4):366–77. [PubMed: 18596266]
20. Tedder TF, Steeber DA, Chen A, Engel P. The selectins: vascular adhesion molecules. *Faseb J* 1995;9(10):866–73. [PubMed: 7542213]
21. Dimitroff CJ, Lechpammer M, Long-Woodward D, Kutok JL. Rolling of human bone-metastatic prostate tumor cells on human bone marrow endothelium under shear flow is mediated by E-selectin. *Cancer Res* 2004;64(15):5261–9. [PubMed: 15289332]
22. Giavazzi R, Foppolo M, Dossi R, Remuzzi A. Rolling and adhesion of human tumor cells on vascular endothelium under physiological flow conditions. *J Clin Invest* 1993;92(6):3038–44. [PubMed: 7504697]
23. Yuan K, Kucik D, Singh RK, Listinsky CM, Listinsky JJ, Siegal GP. Alterations in human breast cancer adhesion-motility in response to changes in cell surface glycoproteins displaying alpha-L-fucose moieties. *Int J Oncol* 2008;32(4):797–807. [PubMed: 18360707]
24. Tremblay PL, Huot J, Auger FA. Mechanisms by which E-selectin regulates diapedesis of colon cancer cells under flow conditions. *Cancer Res* 2008;68(13):5167–76. [PubMed: 18593916]
25. Greenberg AW, Hammer DA. Cell separation mediated by differential rolling adhesion. *Biotechnol Bioeng* 2001;73(2):111–24. [PubMed: 11255159]
26. Rana K, Liesveld JL, King MR. Delivery of apoptotic signal to rolling cancer cells: a novel biomimetic technique using immobilized TRAIL and E-selectin. *Biotechnol Bioeng* 2009;102(6):1692–702. [PubMed: 19073014]
27. Hong S, Lee D, Zhang H, Zhang JQ, Resvick JN, Khademhosseini A, King MR, Langer R, Karp JM. Covalent immobilization of p-selectin enhances cell rolling. *Langmuir* 2007;23(24):12261–8. [PubMed: 17949112]
28. Ramezani A, Hawley RG. Generation of HIV-1-based lentiviral vector particles. *Curr Protoc Mol Biol*. 2002 Chapter 16, Unit 16 22.
29. Nilsson R, Sjogren HO. Antigen-independent binding of rat immunoglobulins in a radioimmunoassay. Solutions to an unusual background problem. *J Immunol Methods* 1984;66(1):17–25. [PubMed: 6607290]
30. Goldman AJ, Cox RG, Brenner H. Slow viscous motion of a sphere parallel to a plane wall--II Couette flow. *Chemical Engineering Science* 1967;22(4):653–660.
31. Kobzdej MM, Leppanen A, Ramachandran V, Cummings RD, McEver RP. Discordant expression of selectin ligands and sialyl Lewis x-related epitopes on murine myeloid cells. *Blood* 2002;100(13):4485–94. [PubMed: 12393554]
32. Zou X, Patil V. R. Shinde, Dagia NM, Smith LA, Wargo MJ, Interliggi KA, Lloyd CM, Tees DF, Walcheck B, Lawrence MB, Goetz DJ. PSGL-1 derived from human neutrophils is a high-efficiency ligand for endothelium-expressed E-selectin under flow. *Am J Physiol Cell Physiol* 2005;289(2):C415–24. [PubMed: 15814589]

33. Brorson SH. Bovine serum albumin (BSA) as a reagent against non-specific immunogold labeling on LR-White and epoxy resin. *Micron* 1997;28(3):189–95. [PubMed: 9332008]
34. Aigner S, Ramos CL, Hafezi-Moghadam A, Lawrence MB, Friederichs J, Altevogt P, Ley K. CD24 mediates rolling of breast carcinoma cells on P-selectin. *Faseb J* 1998;12(12):1241–51. [PubMed: 9737727]
35. Chen S, Springer TA. An automatic braking system that stabilizes leukocyte rolling by an increase in selectin bond number with shear. *J Cell Biol* 1999;144(1):185–200. [PubMed: 9885254]
36. Sachs L. Control of growth and normal differentiation in leukemic cells: regulation of the developmental program and restoration of the normal phenotype in myeloid leukemia. *J Cell Physiol Suppl* 1982;1:151–64. [PubMed: 7040418]
37. Lawrence MB, Springer TA. Leukocytes roll on a selectin at physiologic flow rates: distinction from and prerequisite for adhesion through integrins. *Cell* 1991;65(5):859–73. [PubMed: 1710173]
38. Atherton A, Born GV. Relationship between the velocity of rolling granulocytes and that of the blood flow in venules. *J Physiol* 1973;233(1):157–65. [PubMed: 4759098]
39. Gout S, Tremblay PL, Huot J. Selectins and selectin ligands in extravasation of cancer cells and organ selectivity of metastasis. *Clin Exp Metastasis* 2008;25(4):335–44. [PubMed: 17891461]
40. Tozeren A, Kleinman HK, Grant DS, Morales D, Mercurio AM, Byers SW. E-selectin-mediated dynamic interactions of breast- and colon-cancer cells with endothelial-cell monolayers. *Int J Cancer* 1995;60(3):426–31. [PubMed: 7530236]
41. Zen K, Liu DQ, Guo YL, Wang C, Shan J, Fang M, Zhang CY, Liu Y. CD44v4 is a major E-selectin ligand that mediates breast cancer cell transendothelial migration. *PLoS ONE* 2008;3(3):e1826. [PubMed: 18350162]
42. Ley K, Laudanna C, Cybulsky MI, Nourshargh S. Getting to the site of inflammation: the leukocyte adhesion cascade updated. *Nat Rev Immunol* 2007;7(9):678–689. [PubMed: 17717539]
43. Stroock AD, Dertinger SK, Ajdari A, Mezic I, Stone HA, Whitesides GM. Chaotic mixer for microchannels. *Science* 2002;295(5555):647–51. [PubMed: 11809963]
44. Kiani MF, Fenton BM, Sporn LA, Siemann DW. Effects of ionizing radiation on the adhesive interaction of human tumor and endothelial cells in vitro. *Clin Exp Metastasis* 1997;15(1):12–8. [PubMed: 9009101]

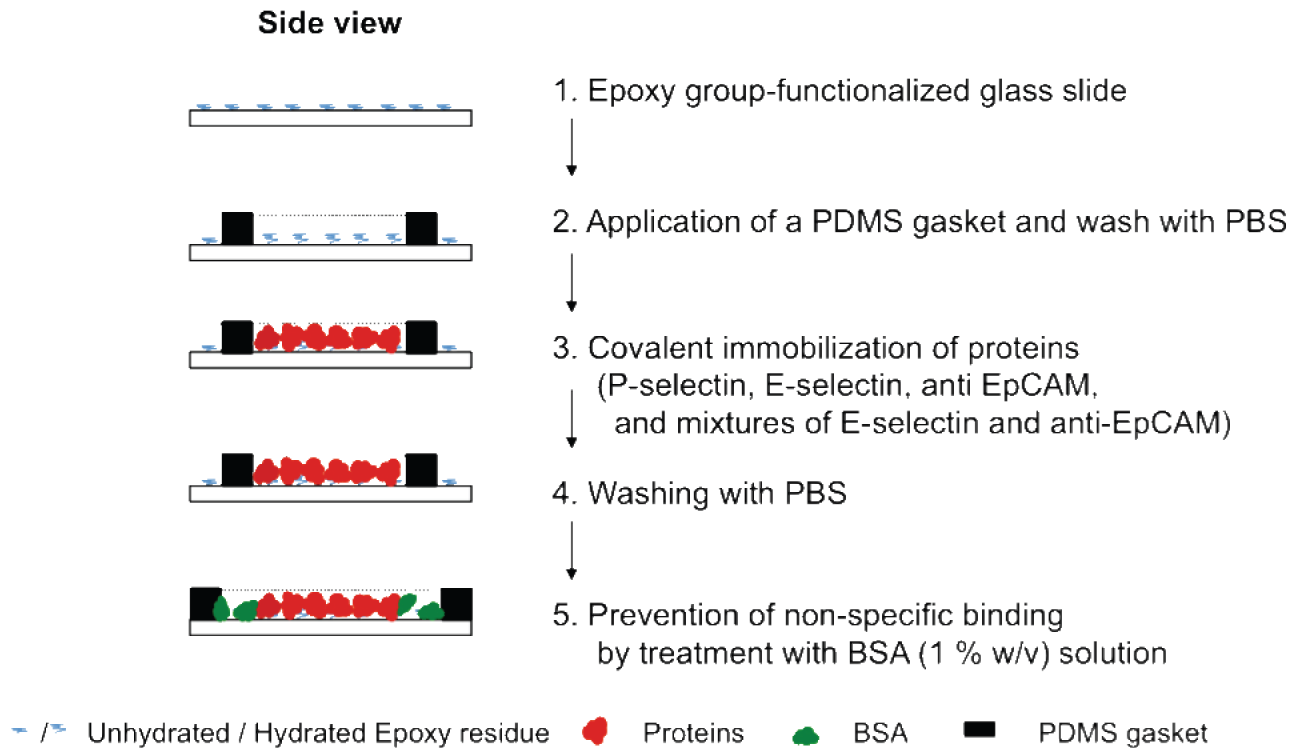


**Figure 1.**  
Surface functionalization by immobilization of proteins.

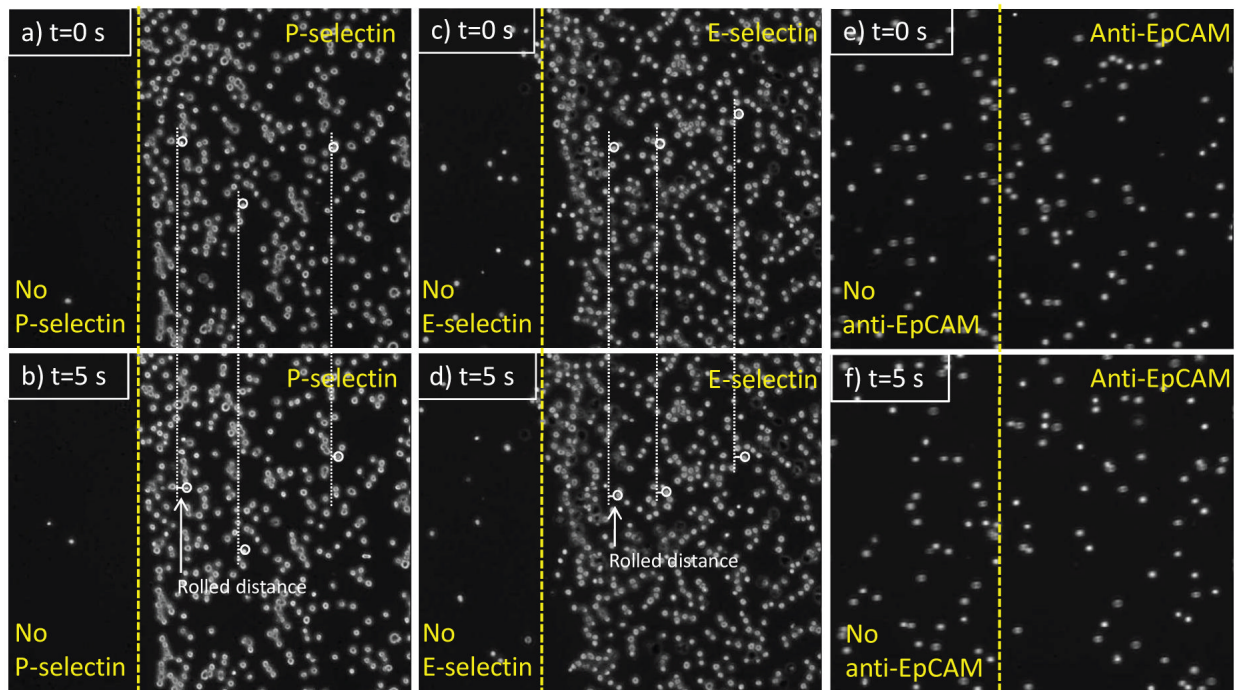


**Figure 2.**

Time-course images of HL-60 cells under shear stress of  $0.32 \text{ dyn/cm}^2$  on (a) and (b) P-selectin, (c) and (d) E-selectin, and (e) and (f) anti-EpCAM-immobilized surfaces. The rolling velocities (mean  $\pm$  standard error,  $n=200$ ) of the cells on P-selectin and E-selectin were  $2.26 \pm 0.28$  and  $2.12 \pm 0.15 \text{ } \mu\text{m/sec}$ , respectively, whereas there was no interaction observed between the cells and anti-EpCAM-coated surface. The cells in the images (e) and (f) are non-interacting flowing cells. Flow direction of the three sets is from left to right.

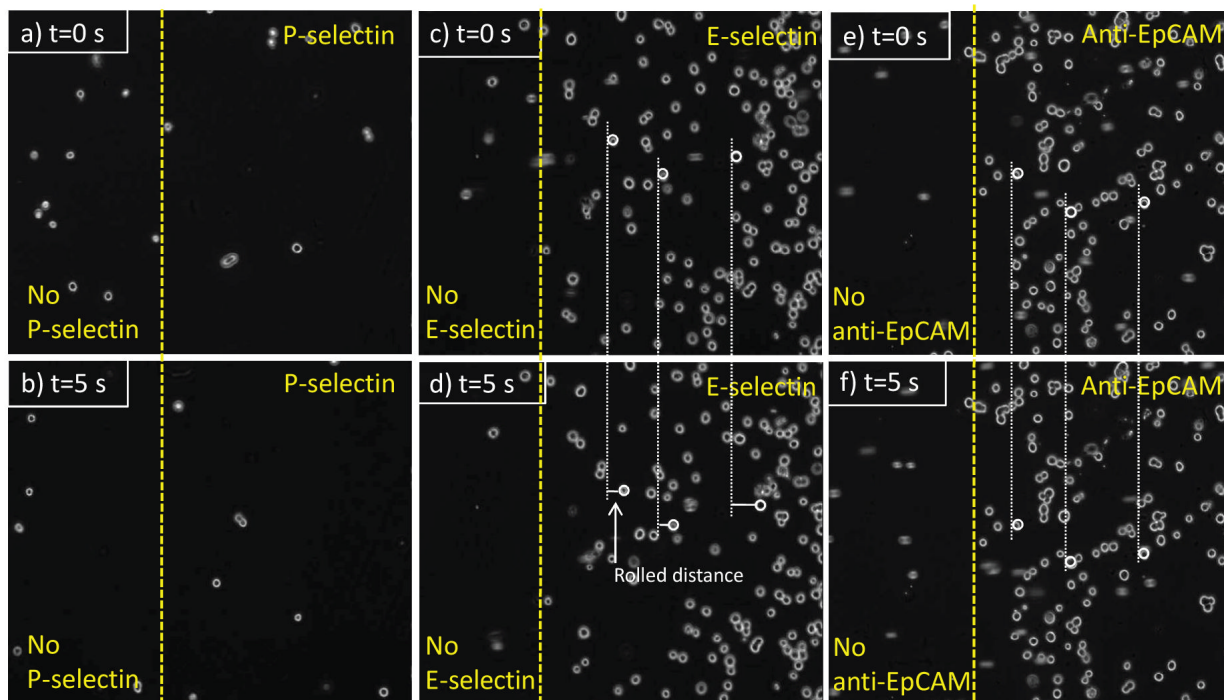


**Figure 3.**

Time-course images of MCF-7 cells under shear stress of  $0.32 \text{ dyn/cm}^2$  on (a) and (b) P-selectin, (c) and (d) E-selectin, and (e) and (f) anti-EpCAM-immobilized surfaces. MCF-7 cells exhibited the rolling behavior on the E-selectin-coated surface ( $4.24 \pm 0.31 \text{ m/sec}$ ) or captured on the anti-EpCAM-coated surface. However, there was no interaction observed between the cells and the P-selectin-coated surface. Flow direction of the three sets is from left to right. All of the rolling dynamic data is represented as mean  $\pm$  standard error ( $n=200$ ).

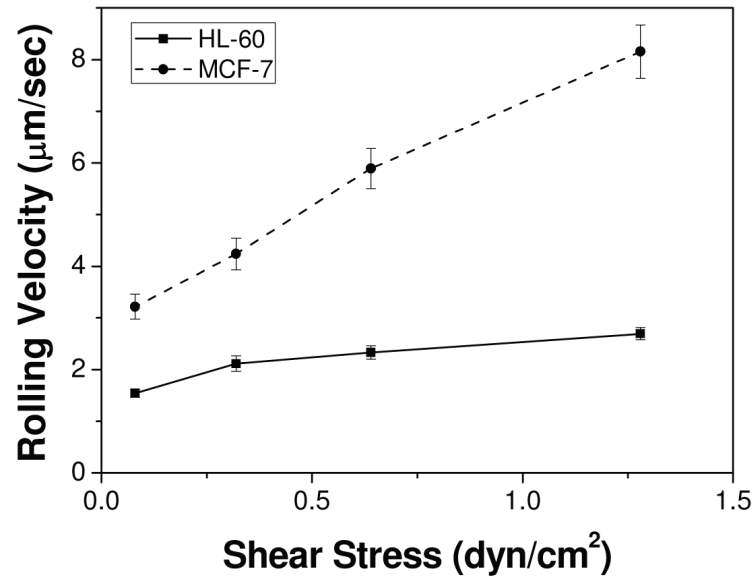


**Figure 4.** Cell rolling velocities of HL-60 and MCF-7 cells on E-selectin-immobilized slides at various shear stresses (0.08 dyn/cm<sup>2</sup>, 0.32 dyn/cm<sup>2</sup>, 0.64 dyn/cm<sup>2</sup>, and 1.28 dyn/cm<sup>2</sup>). Note that the rolling response of HL-60 cells is minimally affected by an increase in shear stress, whereas MCF-7 cells show rolling highly dependent upon shear stress. Error bars: standard error.

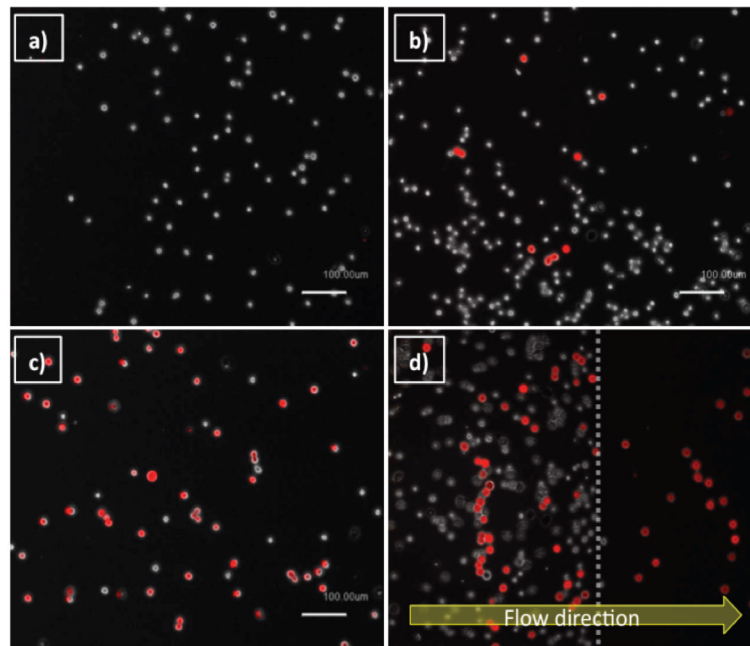


**Figure 5.** Images of HL-60 and DsRED-transfected MCF-7 cells (red cells) on (a) P-selectin, (b) E-selectin, (c) anti-EpCAM, and (d) patterned E-selectin/anti-EpCAM coated surfaces, under shear stress of  $0.32 \text{ dyn/cm}^2$ . The patterned surface with E-selectin and anti-EpCAM shown in (d) achieved efficient isolation of DsRED-transfected MCF-7 (a CTC model: red cells) cells from the mixture with HL-60 (a leukocyte model: white cells), on the anti-EpCAM coated region.

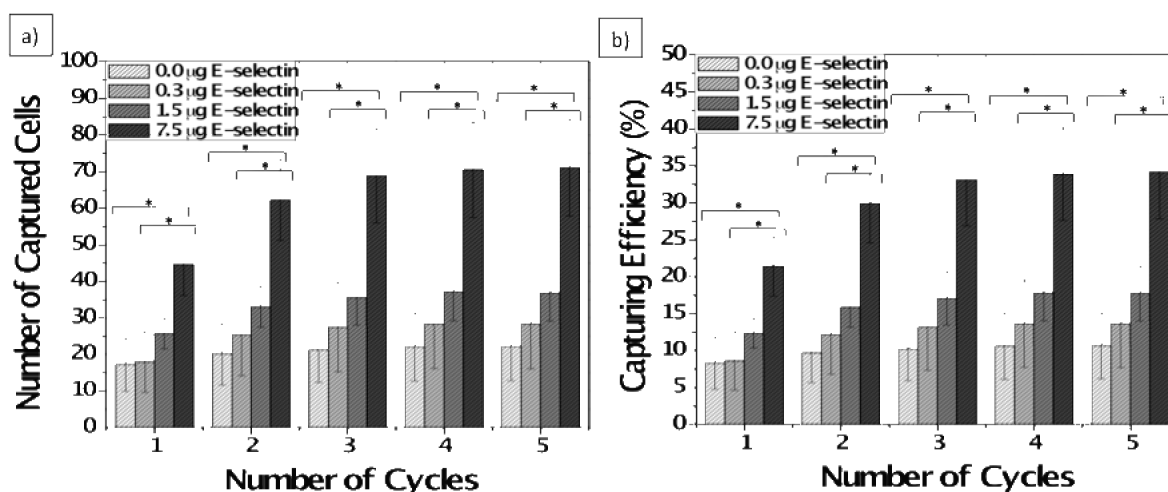


**Figure 6.**

(a) Number of captured cells and (b) capture efficiencies of the surfaces immobilized with the mixtures of anti-EpCAM and E-selectin. The number of DsRED-MCF-7 cells on each surface was counted and the capture efficiency was calculated based on the total number of MCF-7 cells injected into the flow chamber. The flow experiments were performed at a shear stress of  $0.16 \text{ dyn/cm}^2$ . The average capture efficiencies of the surfaces with the mixture of E-selectin and anti-EpCAM were generally higher than those with anti-EpCAM alone. With an increase in E-selectin concentration, the capture efficiency of the surfaces was further enhanced as high as 3-fold. The measured capture efficiencies were compared by statistical analysis using one-factor ANOVA, followed by Fisher's least significant difference (LSD) tests with 95% simultaneous confidence intervals (SPSS software). Error bars: standard error. \*  $p < 0.05$ .

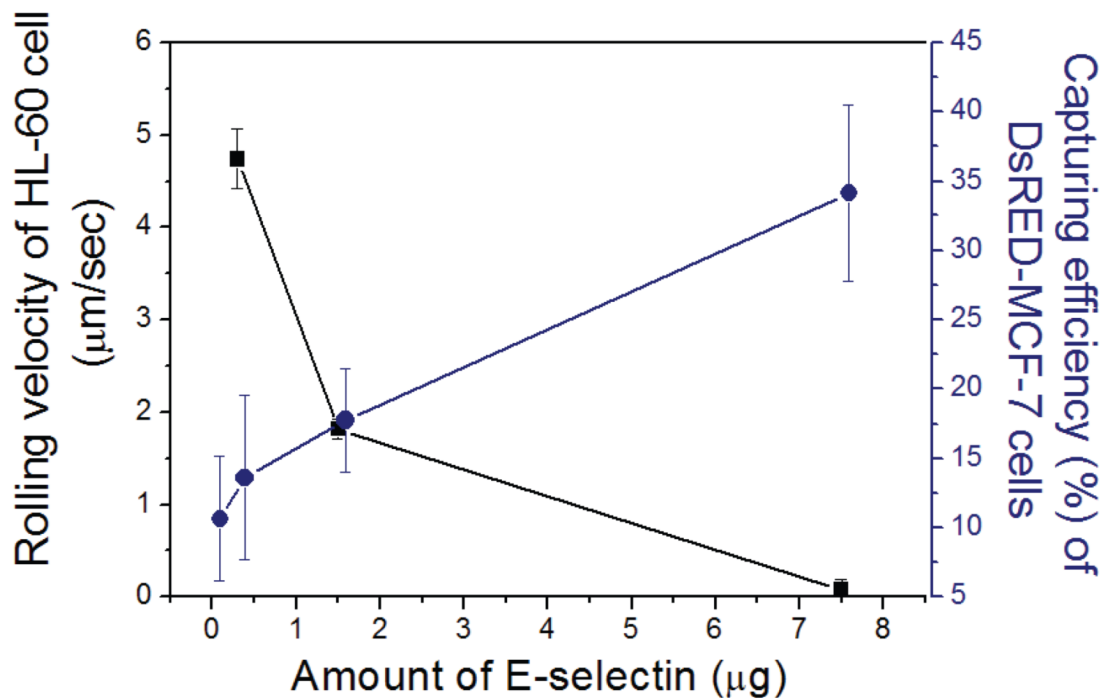


**Figure 7.**

Effect of the amount of E-selectin added to E-selectin/anti-EpCAM mixture on rolling velocity of HL-60 cells and capture efficiency of DsRED-MCF-7 cells. Mixture of the two cell populations (1:1) were injected onto the surfaces co-immobilized with anti-EpCAM and E-selectin under the presence of anti-IgG at a shear stress of  $0.16 \text{ dyn/cm}^2$ . The amount of immobilized E-selectin was increased from 0, 0.3, and 1.5 to 7.5  $\mu\text{g}$ , while the amount of immobilized anti-EpCAM was constant at 1.5  $\mu\text{g}$ . The rolling velocities of HL-60 cells on each slides were  $4.74 \pm 0.32$  (0.3  $\mu\text{g}$ ),  $1.82 \pm 0.10$  (1.5  $\mu\text{g}$ ), and  $0.07 \pm 0.12$  (7.5  $\mu\text{g}$  of E-selectin)  $\mu\text{m/sec}$ . Error bars: standard error.

**Table 1**

Immunostaining results of surfaces immobilized with E-selectin, anti-EpCAM, and mixtures of the two proteins.

	Anti-EpCAM (1.5 $\mu$ g)	E-selectin (1.5 $\mu$ g)	Anti-EpCAM (1.5 $\mu$ g):E-selectin (0.3 $\mu$ g)	Anti-EpCAM (1.5 $\mu$ g):E- selectin (1.5 $\mu$ g)	Anti-EpCAM (1.5 $\mu$ g):E- selectin (7.5 $\mu$ g)
FITC-anti-E- selectin (for E-selectin detection)	-	1	0.04 $\pm$ 0.01	0.66 $\pm$ 0.06	1.31 $\pm$ 0.02
APC-anti- EpCAM (for anti-EpCAM detection)	1	-	0.88 $\pm$ 0.31	0.96 $\pm$ 0.70	0.61 $\pm$ 0.31

Note that all the fluorescence intensities were normalized based on the intensities measured on the surfaces with individual proteins.

**Table 2**

Atomic compositions of functionalized slides with various proteins, as measured by XPS.

	Control (mass conc. %)	E-Selectin (mass conc. %)	Anti-EpCAM (mass conc. %)	Anti-EpCAM 1.5 µg: E- selection 0.3 µg (mass conc. %)	Anti-EpCAM 1.5 µg: E- selection 1.5 µg (mass conc. %)	Anti-EpCAM 1.5 µg: E- selection 7.5 µg (mass conc. %)
C 1s	11.3	21.6	26.2	32.5	40.2	36.9
N 1s	0.0	5.4	2.6	3.5	4.6	6.5
O 1s	59.7	51.9	39.2	43.3	35.5	40.7
Si 2p	29.0	21.1	32.0	20.7	19.7	15.9
N/C ratio	0.0	0.3	0.1	0.1	0.1	0.2
C/O ratio	0.2	0.4	0.7	0.8	1.1	0.9